Hue University Journal of Science: Natural Science
Vol. 135, No. 1B, 27–35, 2026

pISSN 1859-1388
eISSN 2615-9678

Novel MIL-53(Fe)-encapsulated gelatinous boehmite granules and their enhanced photocatalytic performance towards tetracycline

Thi Minh Nguyet Bui[1], Van Hung Nguyen[1], Cao Duy An Nguyen[2], Ngoc Bich Nguyen[1], The Ky Vo[3*]

[1] Faculty of Natural Sciences and Education, Dong Thap University, Dongthap, Vietnam
[2] Quoc Hoc Hue High School, Hue, Vietnam
[3] Faculty of Chemical Engineering, Industrial University of Ho Chi Minh City, Ho Chi Minh City, Vietnam

* Correspondence to The Ky Vo <votheky@iuh.edu.vn>

(*Received: 28 January 2026; Revised: 23 March 2026; Accepted: 23 March 2026*)

Abstract. Developing materials with high photocatalytic activity and easy recovery remains a challenge in industry. In this work, MIL-53(Fe) crystal powder was effectively encapsulated within gelatinous boehmite to produce millimetre-scale AlOOH@MIL-53(Fe) granules using the oil-drop method. The materials were utilised for the photodegradation of tetracycline (TC). These granules underwent detailed characterisation by SEM, FT-IR, XRD, N_2 sorption, TGA, and UV-Vis DRS techniques. The resulting granular composites exhibited improved porosity and visible-light absorption. Photocatalytic testing under energy-efficient visible LED light demonstrated that the AlOOH@MIL-53(Fe) granules achieved a removal efficiency of 93% for TC, higher than that of the original MOF (82%) and the AlOOH granules without loaded MOF (54%). Kinetic analysis indicated that the photodegradation of TC followed a pseudo-second-order model, with rate constants in the following decreasing order: AlOOH@MIL-53(Fe) (0.0021 $mg^{-1}.L.min^{-1}$), MIL-53(Fe) (0.00074 $mg^{-1}.L.min^{-1}$), and AlOOH(0.00016 $mg^{-1}.L.min^{-1}$). Notably, the developed granules are easy to recover and retain suitable reusability in photocatalytic processes, highlighting their significant potential for real-world wastewater treatment applications.

Keywords: photocatalytic, MIL-53(Fe), boehmite, visible LED light, tetracycline

1 Introduction

Water pollution is a serious global problem. The release of pollutants with varying levels of toxicity poses a major challenge for scientists [1, 2]. Pharmaceutical substances such as antibiotics, analgesics, and anti-inflammatory drugs are among the most common contaminants in water bodies. The overuse and uncontrolled disposal of antibiotics into the environment lead to their accumulation in ecosystems, as most antibiotics are stable and non-biodegradable [3, 4]. Therefore, finding an effective way to remove antibiotics from wastewater is an substantial challenge.

Advanced oxidation processes, including photolysis, semiconductor-based photocatalysis, and ozonation, have been used to transform and remove antibiotics from aquatic ecosystems [5, 6]. Among these methods, the advanced oxidation process is regarded as a sustainable approach for degrading pharmaceutical compounds, utilising highly reactive and oxidising species. It offers distinct advantages because it uses natural light as the primary driver, reduces secondary pollution, and is cost-effective. Various types of photocatalysts have been studied for the photodegradation of antibiotics. Conventional semiconductors, such as TiO_2, Ag_3PO_4, Fe_3O_4, and CdS, have shown potential for photocatalytic degradation of organic contaminants [7–9]. However, these materials have certain limitations because of their small surface area and pore volume. Moreover, the direct use of these colloidal semiconductors has created severe secondary pollution and increased costs, as they tend to readily disperse into the environment during processing.

Recently, metal-organic frameworks (MOFs) have garnered increasing interest as photocatalysts because of their tunable porous structures and substantial surface areas [10–14]. Furthermore, the MOF framework can be modified by substituting metal centres and organic ligands with those containing different functional groups to enhance catalytic performance. Among known MOF structures, MIL-53(Fe), composed of Fe^{3+} clusters and terephthalate ligands, exhibits responsiveness to visible light owing to its low bandgap energy (<3.1 eV) [15, 16]. MIL-53(Fe)-based materials have been developed for photocatalytic applications. For instance, the Ag_3PO_4/MIL-53(Fe) hybrid demonstrated high photocatalytic activity against antibiotics [17]. Additionally, MIL-53(Fe)/Sn_3O_4 nanosheets were synthesised and shown to be effective in degrading organic pollutants [18]. To date, much research has concentrated on improving the photocatalytic activity of MIL-53(Fe) and related MOF-based materials. However, limited efforts have been directed towards designing MOF structures that balance high catalytic activity with facile recovery, aiming to minimise losses and prevent secondary pollution.

This study involved encapsulating MIL-53(Fe) crystals within gelatinous boehmite to produce AlOOH@MIL-53(Fe) granules approximately 1~2 mm in diameter by using the oil-drop method. These granules underwent detailed characterisation with SEM, FT-IR, XRD, N_2 sorption, TGA, and UV-Vis DRS techniques. The resulting granular composites exhibited improved visible-light absorption. Photocatalytic testing under energy-efficient visible LED light demonstrated that the AlOOH@MIL-53(Fe) granules achieved higher degradation efficiency for tetracycline than the pure MOF. Notably, the granules are easy to recover and demonstrate good reusability in photocatalytic processes, highlighting their great potential for real-world wastewater treatment applications.

2 Experimental

2.1 Materials and instrument

Instrument

The X-ray diffraction analysis of the granules was conducted by using an X-ray diffraction analyser (XRD; Miniflex 600, Rigaku, Japan) with Cu Kα radiation (λ = 1.54 Å). The morphology of the materials was examined by employing high-resolution field-emission scanning electron microscopy (FE-SEM; Leo Supra 55, Carl Zeiss, Germany). Fourier Transform Infrared spectra were identified by using an FT-IR spectrometer (Tensor 27, Bruker, Germany). The sample's N_2 sorption measurements were performed via N_2 porosimetry (Tristar 3020, Micromeritics, USA) at 77 K. Thermal stability was evaluated through thermogravimetric analysis (TGA; Q50, TA Instruments, USA) under a nitrogen atmosphere. UV-Vis diffuse reflectance spectra (UV-Vis DRS) were recorded by utilising a Shimadzu UV-2600 spectrometer.

Chemicals

Iron (III) chloride hexahydrate ($FeCl_3{\cdot}6H_2O$, 98%), benzene-1,4-dicarboxylic acid (H_2BDC, 98%), and Aluminum nitrate nonahydrate ($Al(NO_3)_3{\cdot}9H_2O$, 97%) were purchased from Sigma-Aldrich. Dimethylformamide (DMF) and NH_3 were obtained from Daejun company (Korea). All chemicals were used as received without further purification.

pISSN 1859-1388
eISSN 2615-9678

2.2 Material synthesis

Preparation of MIL-53(Fe)

MIL-53(Fe) frameworks were synthesised via solvothermal synthesis. Typically, 1.5 g of $FeCl_3·6H_2O$ and 0.80 g of benzene-1,4-dicarboxylic acid (H_2BDC) were dispersed in 45 mL of DMF under vigorous stirring. The mixture was poured into a Teflon-lined steel autoclave (100 mL) and heated to 150 °C for 24 hours. After reaction, the mixture was centrifuged to collect a yellow powder, which was subsequently washed twice with DMF and twice with ethanol. The sample was then heated at 115 °C under vacuum to evacuate before use.

Preparation of AlOOH@MIL-53(Fe)

AlOOH@MIL-53(Fe) granules with a diameter of 1–2 mm were prepared with the oil-drop method, as described in our previous work [19]. A boehmite sol (2 M) was prepared by hydrolysing $Al(NO_3)_3·9H_2O$ in an NH_3 solution, following our previous work [20]. For the preparation of granules, 25 mL of boehmite sol was sonicated and stirred for 30 minutes. Subsequently, 0.3 g of MIL-53(Fe) powder was added to the mixture. It was then sonicated and stirred for a further 30 minutes. Afterwards, the solution was slowly dropped into a glass column filled with paraffin oil at the top and ammonia solution at the bottom. The granules were collected, washed several times with ethanol, and dried at 70 °C for 12 hours. The resulting granules were designated as AlOOH@MIL-53(Fe). The AlOOH granules were prepared with the same procedure without adding the MOF crystal.

2.3 Photodegradation of tetracycline

The prepared materials were used to photodecompose tetracycline under visible LED light. In each run, the catalyst was dispersed in 50 mL of a contaminant solution (25 mg/L, pH ~5) in a photoreactor with continuous stirring. The suspension was magnetically stirred in the dark for 90 minutes to reach absorption equilibrium. Subsequently, the mixture was exposed to the light source. At each time interval, 2 mL of the reaction solution was withdrawn and filtered to obtain a solution for analysis with a UV-Vis spectrophotometer.

3 Results and discussion

3.1 Characteristics

Fig. 1 displays optical images of the produced granules. MIL-53(Fe) appears as a yellow powder (Fig. 1a). The granules encapsulated with MIL-53(Fe) powder exhibit the characteristic brownish-yellow colour of MIL-53(Fe) (Fig. 1b). Morphology analyses show that the pure MOF appears as an octahedral diamond-shaped form with diameters of 0.5~1.5 μm (Fig. 1c). SEM images of the interior of the AlOOH@MIL-53(Fe) granules indicate that crystalline MOFs are encapsulated within the granules (Fig. 1d). EDX dot-mapping demonstrates a uniform distribution of elements C, Al, O, and Fe within the granular composites (Figs. 1e–h).

Fig. 2a depicts the XRD patterns of the prepared structures. The bare MOF sample exhibits prominent diffraction peaks at 9.18, 9.77, 10.69, and 21.42°, which are clearly visible and correspond well to those previously reported for the MIL-53(Fe) framework [15, 21]. The AlOOH granules exhibit peaks at 2θ ~13.71, 38.21, 48.82, and 88°, which are characteristics of pseudo-boehmite [22, 23]. These peaks are slightly weakened and shifted upon incorporation of MOF crystals into the boehmite matrix. Furthermore, the absence of MOF signals in the granules proves that MOF crystals are well encapsulated within the AlOOH granules. The FT-IR spectrum of the powder MIL-53(Fe) and the AlOOH@MIL-53(Fe) granules are presented in Fig. 2b. MIL-53(Fe) displays a broad band at 3400 cm^{-1}, resulting from the vibration of –OH groups from physically adsorbed water. The bands at 1600 cm^{-1} and 1200 cm^{-1} are attributed to the stretching of the C=O and C–O–C linkages of the ligands, respectively [24–26]. Lower wavenumber bands ranging from 600 to 900 cm^{-1} are characteristic of benzene rings, and the signal at 540 cm^{-1} is assigned to Fe–O bonds [4, 25]. These bands are also present in AlOOH@MIL-53(Fe) but with reduced intensities. The boehmite granules display a broad band at 3400 cm^{-1} because of the stretching of –OH groups, while the lower modes at approximately 1064 cm^{-1} and 480 cm^{-1} are attributed to bending modes of the Al–O bonds in boehmite [22, 27]. The spectra of the composite granules show diminished intensities and shifted positions of the Fe–O and Al–O bands, suggesting that boehmite can be incorporated into the MIL-53(Fe) framework. Thermogravimetric analysis was used to assess the thermal stability of the fabricated granules, as shown in Fig. 2c. Pure MIL-53(Fe) experienced a minor weight loss from 120 to 250 °C caused by solvent evaporation, while a significant weight loss near 380 °C resulted from framework decomposition [15, 28]. The TGA analysis of the AlOOH granules indicates a gradual weight loss beginning at 200 °C, attributable to the dehydration of γ-AlOOH [29, 30]. The TGA results for AlOOH@MIL-53(Fe) granules demonstrate improved thermal stability compared with that of the AlOOH sample, reflecting the interaction between MIL-53(Fe) frameworks and boehmite, which forms a composite structure. Additionally, N_2 adsorption-desorption isotherms of the fabricated adsorbents are shown in Fig. 2d. Incorporating MIL-53(Fe) into the boehmite spheres enhances the N_2 sorption capacity. The BET surface areas of MIL-53(Fe) and AlOOH are approximately 330 m^2/g and 351 m^2/g, respectively; and the corresponding pore volumes are 0.29 and 0.51 cm^3/g. The granular AlOOH@MIL-53(Fe) composite has a surface area and a pore volume of 370 m^2/g and 0.62 cm^3/g, respectively (Table 1).

The optical properties of the materials were examined by using UV-Vis DRS spectra (Fig. 2e). The AlOOH granules exhibited an absorption edge at around 390 nm, while that of pristine MIL-53(Fe) is at nearly 450 nm. It is clear that the absorption edge of the granular composite AlOOH@MIL-53(Fe) shifted significantly towards the visible spectrum, indicating that MIL-53(Fe) was effectively integrated into the supporting AlOOH matrix and could generate defective structures that enhanced the light absorption of the composite.

Fig. 1. Optical images of (a) MIL-53(Fe) and (b) AlOOH@MIL-53(Fe); SEM images of (c) MIL-53(Fe) and (d) the interior region of AlOOH@MIL-53(Fe) granules; (e–k) EDX dot map analyses of C, O, Al, and Fe in the AlOOH@MIL-53(Fe) granules

pISSN 1859-1388
eISSN 2615-9678

Table 1. Textural properties of the materials

Sample	BET surface area, m^2/g	Total pore volume, cm^3/g
MIL-53(Fe)	330	0.29
AlOOH	351	0.51
AlOOH@MIL-53(Fe)	370	0.62

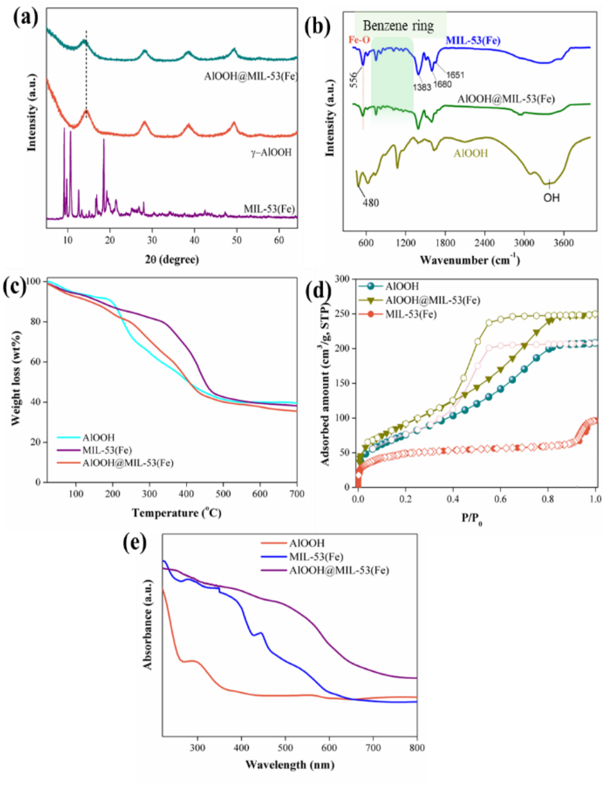

Fig. 2. Characteristics of the synthesised materials: (a) XRD patterns; (b) FT-IR; (c) TGA analyses; (d) N_2 sorption-desorption; (e) UV-Vis DRS spectrum

3.2 Photocatalytic degradation of tetracycline

Fig. 3a illustrates the photocatalytic degradation efficiency of TC with the synthesised materials under visible LED light. The granular AlOOH material achieved 54% removal efficiency after 120 minutes, indicating a limited effectiveness. It is apparent that the AlOOH system adsorbs the contaminant solely, as it is inactive under visible light. The pristine MIL-53(Fe) powder degraded 82% of TC. Notably, the AlOOH@MIL-53(Fe) granules achieved a TC removal efficiency of 93% after 120 minutes. The UV-Vis spectra's intensities of the reaction solutions gradually decreased, confirming the degradation of TC over the granular catalysts (Fig. 3b). Such an enhancement over the AlOOH@MIL-53(Fe) granules may be ascribed to the synergistic effect of incorporating MIL-53(Fe) frameworks into the AlOOH matrix, which possesses numerous functional groups that interact more efficiently with tetracycline. Furthermore, the formation of interfacial structures between AlOOH and MIL-53(Fe), which, as mentioned previously, augmented light absorption, also facilitated photocatalytic reactivity. The prepared AlOOH@MIL-53(Fe) granules exhibited greater TC removal efficiency than previous catalysts, such as La-doped $ZnTiO_3$ (~80%) [31] and BVO@CdS (~88%) [32]. The kinetic analyses of the degradation process are conducted utilising pseudo-first-order (Eq. 1) and pseudo-second-order kinetics (Eq. 2):

$$\ln \frac{C_0}{C_t} = k_1 t \quad (1)$$

$$\frac{1}{C_t} = \frac{1}{C_0} + k_2 t \quad (2)$$

where C_0 (mg/L) and C_t (mg/L) are the initial concentration and the concentration of TC at time t; k_1 (min^{-1}) and k_2 ($mg^{-1}.L.min^{-1}$) are the first-order and second-order rate constants, respectively.

Figs. 3c–d show the kinetic plots, and the corresponding fitting parameters are listed in Table 2. The degradation of the TC modelled with the second-order kinetic model had higher R^2 values than those from the first-order model. Consequently, it can be inferred that photodegradation follows the second-order kinetic model. Accordingly, the degradation rates of TC over the catalysts follow the sequence: AlOOH@MIL-53(Fe) (0.0021 $mg^{-1}.L.min^{-1}$) > MIL-53(Fe) (0.00074 $mg^{-1}.L.min^{-1}$) > AlOOH(0.00016 $mg^{-1}.L.min^{-1}$).

DOI: 10.26459/hueunijns.v135i1B.8271

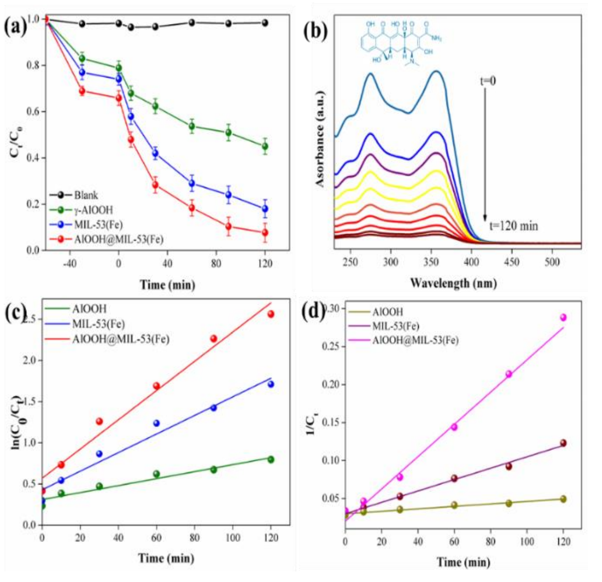

Fig. 3. Photodegradation of TC over the prepared materials: (a) Removal efficiency, (b) Time-dependent UV-Vis spectrum of reaction solution; fitting kinetic models (c) pseudo-first order model; (d) pseudo-second order model

Table 2. Fitting kinetic parameters for TC photodegradation

Sample	Pseudo-first-order		Pseudo-second-order	
	k_1, min^{-1}	R^2	k_2, $mg^{-1}.L.min^{-1}$	R^2
AlOOH	0.0042	0.957	0.00016	0.971
MIL-53(Fe)	0.0112	0.976	0.00074	0.994
AlOOH@MIL-53(Fe)	0.0187	0.961	0.00210	0.985

3.3 Reusability and photocatalytic mechanism studies

Reusability is a crucial factor in evaluating the catalysts. Here, the AlOOH@MIL-53(Fe) granules were collected after each use. The catalysts were then immersed in deionised water and ethanol, and dried at 70 °C for 10 hours before being reused as regenerated catalysts. After three cycles, the photodegradation efficiency reached nearly 82%, compared with that of the as-prepared granules [Fig. 4a]. This occurs because TC and intermediates are strongly bound to the granules, thereby inactivating active sites. Overall, the produced photocatalytic granules are easily recovered without loss and remain stable after the treatment process.

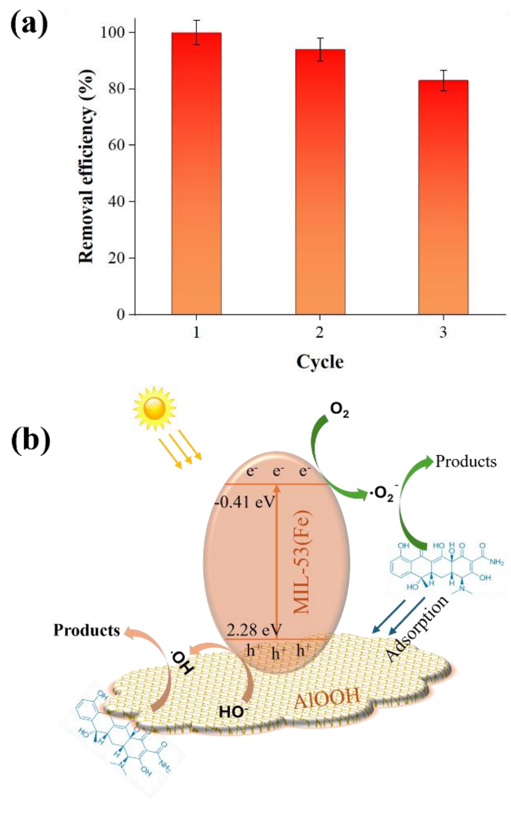

Fig. 4. (a) Reusability test and (b) the proposed photocatalytic degradation of TC over the AlOOH@MIL-53(Fe)

The photocatalytic mechanism of the prepared AlOOH@MIL-53(Fe) granules can be explained via their bandgap structure. As discussed previously, the supporting boehmite not only aids in encapsulating the MOF crystal into the granules but also provides additional mesopores and hydroxyl groups, which attract TC molecules. The MIL-53(Fe) has the conduction band (CB) potential of –0.41 eV [33]. Thus, with regard to the above UV-Vis DRS data, the valence band (VB) of MIL-53(Fe) is about 2.28 eV. Therefore, the adsorbed O_2 can be reduced to $\cdot O_2^-$

pISSN 1859-1388
eISSN 2615-9678

because of the reduction potential of $O_2/{\cdot}O_2^{-}$ (−0.33 eV vs NHE) [34]. Meanwhile, the photo-induced h^+ at the VB of MIL-53(Fe) can convert OH^- to ·OH because the potential of $\cdot OH/OH^-$ is about +1.99 eV vs NHE [35]. Based on the discussion, we illustrated the general photodegradation of TC over the granules in Fig. 4b.

4 Conclusions

Millimetre-scale MIL-53(Fe)-encapsulated gelatinous boehmite granules were successfully produced with the oil-drop method. The granules demonstrated increased porosity and enhanced light adsorption. The AlOOH@MIL-53(Fe) catalyst achieved a high photodegradation efficiency of 93% towards tetracycline after 120 minutes under visible light. The degradation followed the second-order kinetic model with a rate constant of 0.0021 $mg^{-1}.L.min^{-1}$. Notably, the granules were easily recovered and maintained good regenerability throughout the process. The results indicate that encapsulating colloidal MOF crystals with gelled bohmite could be a promising strategy to broaden their industrial applications.

Acknowledgement

This research is supported by the project B2024-SPD-06.

References

1. Mishra P, Tripathi G, Mishra V, Ilyas T, Irum, Firdaus S, et al. Antibiotic contamination in wastewater treatment plant effluents: Current research and future perspectives. Environmental Nanotechnology, Monitoring & Management. 2025;23:101047.
2. Barathe P, Kaur K, Reddy S, Shriram V, Kumar V. Antibiotic pollution and associated antimicrobial resistance in the environment. Journal of Hazardous Materials Letters. 2024;5:100105.
3. He X, Nguyen V, Jiang Z, Wang D, Zhu Z, Wang WN. Highly-oriented one-dimensional MOF-semiconductor nanoarrays for efficient photodegradation of antibiotics. Catalysis Science and Technology. 2018;8(8):2117-23.
4. Vo TK, Kim J. Facile synthesis of magnetic framework composite $MgFe_2O_4$@UiO-66(Zr) and its applications in the adsorption–photocatalytic degradation of tetracycline. Environmental Science and Pollution Research. 2021;28(48):68261-75.
5. Abdi J, Hadipoor M, Hadavimoghaddam F, Hemmati-Sarapardeh A. Estimation of tetracycline antibiotic photodegradation from wastewater by heterogeneous metal-organic frameworks photocatalysts. Chemosphere. 2022;287:132135.
6. Yang X, Chen Z, Zhao W, Liu C, Qian X, Zhang M, et al. Recent advances in photodegradation of antibiotic residues in water. Chemical Engineering Journal. 2021;405:126806.
7. Anucha CB, Altin I, Bacaksiz E, Stathopoulos VN. Titanium dioxide (TiO_2)-based photocatalyst materials activity enhancement for contaminants of emerging concern (CECs) degradation: In the light of modification strategies. Chemical Engineering Journal Advances. 2022;10:100262.
8. Jie L, Gao X, Cao X, Wu S, Long X, Ma Q, et al. A review of CdS photocatalytic nanomaterials: Morphology, synthesis methods, and applications. Materials Science in Semiconductor Processing. 2024;176:108288.
9. Sabar S, Jamil AM, Zhao Y, Md Yusof EN, Schneider R, Mohamed AR, et al. Construction of Fe_3O_4/ZnO heterostructure photocatalysts derived from Fe-doped ZIF-8 for enhanced photocatalytic degradation of tetracycline and hydrogen peroxide production. New Journal of Chemistry. 2025;49(20):8267-78.
10. Swetha S, Janani B, Khan SS. A critical review on the development of metal-organic frameworks for boosting photocatalysis in the fields of energy and environment. Journal of Cleaner Production. 2022;333:130164.
11. Vo TK, Kim J, Park J, Dao DQ, Truong HB. Aminobenzoate-defected UiO-66(Zr)–NH_2 frameworks: Scalable synthesis and characterizations for adsorptive denitrogenation from model fuel. Chemical Engineering Journal. 2024;481:148570.

12. Zeggai Fz, Ait-Touchente Z, Bachari K, Elaissari A. Investigation of Metal-Organic Frameworks (MOFs): Synthesis, Properties, and Applications - An In-Depth Review. Chemical Physics Impact. 2025;10:100864.

13. Minh Nguyet Bui T, Ky Vo T, Hoang Yen Phuong N, Hung Nguyen V, Cuong Nguyen V, Hung Nguyen Q, et al. Fe(III)-incorporated UiO-66(Zr)–NH2 frameworks: Microwave-assisted scalable production and their enhanced photo-Fenton degradation catalytic activities. Separation and Purification Technology. 2025;355:129723.

14. Vo TK, Phuong NHY, Nguyen VC, Quang DT. ZIF-67 grafted-boehmite-PVA composite membranes with enhanced removal efficiency towards Cr(VI) from aqueous solutions. Chemosphere. 2023;341:139996.

15. Li A, Yang X, Chen J. A novel route to size-controlled MIL-53(Fe) metal–organic frameworks for combined chemodynamic therapy and chemotherapy for cancer. RSC Advances. 2021;11(18):10540-7.

16. Shen X, Yu Z, Yang Y, Feng Q, Yang S, Liu S, et al. Visible-NIR responsive Ag_2O couple with MIL-53(Fe) on CS as S-scheme photocatalyst for efficient simultaneous removal of Cr(VI) and norfloxacin. Chemical Engineering Journal. 2024;498:155201.

17. Xie L, Yang Z, Xiong W, Zhou Y, Cao J, Peng Y, et al. Construction of MIL-53(Fe) metal-organic framework modified by silver phosphate nanoparticles as a novel Z-scheme photocatalyst: Visible-light photocatalytic performance and mechanism investigation. Applied Surface Science. 2019;465:103-15.

18. Yuan N, Zhang X, Li B, Chen T, Yang X. Energy-Efficient MIL-53(Fe)/Sn_3O_4 Nanosheet Photocatalysts for Visible-Light Degradation of Toxic Organics in Wastewater. ACS Applied Nano Materials. 2023;6(11):9159-74.

19. Nguyen THA, Van Hung P, Tran HL, Nguyen MQ, Khue VT, Vo TK. Plasmonic Ag-AgCl nanostructures decorated polyvinyl alcohol-boehmite@ZIF-67 granules with enhanced photocatalytic activities toward textile dye and Cr(VI). Colloids and Surfaces A: Physicochemical and Engineering Aspects. 2025;710:136296.

20. Bui TMN, Nguyen VT, Dang THN, Nguyen VC, Nguyen HM, Vo TK. Novel ZIF-8/Ag-AgCl-supported AlOOH-PVA membrane with enhanced visible-light-driven photodegradation of antibiotics. Journal of Molecular Structure. 2026;1355:145035.

21. Veisi B, Lorestani B, Sobhan Ardakani S, Cheraghi M, Tayebi L. Post synthetic modification of magnetite @MIL-53(Fe)-NH2 core-shell nanocomposite for magnetic solid phase extraction of ultra-trace Pd(II) ions from real samples. International Journal of Environmental Analytical Chemistry. 2024;104(5):1092-109.

22. Vo TK, Park H-K, Nam C-W, Kim S-D, Kim J. Facile synthesis and characterization of γ-AlOOH/PVA composite granules for Cr(VI) adsorption. Journal of Industrial and Engineering Chemistry. 2018;60:485-92.

23. The Ky V. Spray pyrolysis synthesis of mesoporous γ-AlOOH and γ-Al_2O_3 microspheres and their properties for Cr (VI) adsorption. International Journal of Environmental Analytical Chemistry. 2024;104(3):584-604.

24. Vo TK, Kim J, Vu TH, Nguyen VC, Quang DT. Creating Cu(I)-decorated defective UiO-66(Zr) framework with high CO adsorption capacity and selectivity. Separation and Purification Technology. 2022;283:120237.

25. Lee JH, Ahn Y, Kwak S-Y. Facile Sonochemical Synthesis of Flexible Fe-Based Metal–Organic Frameworks and Their Efficient Removal of Organic Contaminants from Aqueous Solutions. ACS Omega. 2022;7(27):23213-22.

26. Zhang Z, Zhao K, Li X, Lin S, Li H. The engineering of surface plasmon resonance and up-conversion to improve the photocatalytic performance of MIL-53(Fe) over the full solar spectrum. Journal of Materials Science. 2020;55(3):997-1011.

27. Vo TK, Le VN, Quang DT, Kim J. Facile synthesis of spray pyrolysis-derived CuCl/γ-Al_2O_3 microspheres and their properties for CO adsorption and CO/CO_2 separation. Microporous and Mesoporous Materials. 2021;321:111132.

28. Abdollahi B, Salari D, Zarei M. Synthesis and characterization of magnetic Fe_3O_4@SiO_2-MIL-53(Fe) metal-organic framework and its application for efficient removal of arsenate from surface and groundwater. Journal of Environmental Chemical Engineering. 2022;10(2):107144.

29. Singh J, Dutta PK. Antibacterial and Physiochemical Behavior of Prepared Chitosan/pyridine-3,5-di-carboxylic Acid Complex for Biomedical Applications. Journal of Macromolecular Science, Part A. 2011;48(3):246-53.

pISSN 1859-1388
eISSN 2615-9678

30. Alamri AA, Borik RMA, El-Wahab AHFA, Mohamed HM, Ismail KS, El-Aassar MR, et al. Synthesis of Schiff bases based on Chitosan, thermal stability and evaluation of antimicrobial and antitumor activities. Scientific Reports. 2025;15(1):892.

31. Huang C-W, Chen R-A, Chen W-Y, Nguyen V-H, Lin K-YA, Lasek J. Manipulating and Revealing the Roles of La and Zr Dopants into $ZnTiO_3$ Perovskite Toward Heterogeneous Photocatalytic Degradation of Tetracycline Under Visible Light Irradiation. Topics in Catalysis. 2023;66(1):34-40.

32. Liu K, Ran MJ, Li ZR, Huang YF, Jiang ZY, Li WY, et al. CdS QDs grown on ellipsoidal BiVO4 for efficient photocatalytic degradation of tetracycline. Dalton Transactions. 2024;53(18):8011-9.

33. Huang W, Liu N, Zhang X, Wu M, Tang L. Metal organic framework g-C3N4/MIL-53(Fe) heterojunctions with enhanced photocatalytic activity for Cr(VI) reduction under visible light. Applied Surface Science. 2017;425:107-16.

34. Kong X, Chang K, Tao X, Huang L. Oxygen vacancy and Z-scheme heterojunction cooperate to promote visible light nitrogen photofixation. Chemical Engineering Journal. 2023;475:146159.

35. Mayyahi AA, Sekar A, Rajendran S, Sigdel S, Lu L, Wang J, et al. Hierarchical TiO_2-g-C_3N_4 photocatalyst with purification effect for NOx oxidation under cyan light. Journal of Photochemistry and Photobiology A: Chemistry. 2023;444:114965.